Available online at www.sciencedirect.com

ScienceDirect

Procedia IUTAM 15 (2015) 108 – 115

Procedia IUTAM

www.elsevier.com/locate/procedia

IUTAM Symposium on Multiphase flows with phase change: challenges and opportunities, Hyderabad, India (December 08 – December 11, 2014)

Natural Convection Driven Evaporation from a water surface

Navneet Kumar[a]* and Jaywant H Arakeri[b]

[a]*Dept. of Mechanical Engg., Indian Institute of Science, Bangalore-560012, India*
[b]*Dept. of Mechanical Engg., Indian Institute of Science, Bangalore-560012, India*

Abstract

We measure evaporation rates from water kept in an insulated tank and which is at a temperature higher than the ambient. Different schemes are used to obtain different temperature profiles in the water layer: a) water is heated from bellow, b) water left to cool after being heated, c) water heated from above with an IR heater, d) water heated from above in a very shallow tank. The idea of having these different schemes is to check the role of water side convection on evaporation rates. In cases a) and b) unstable stratification causes convection; in case c) we have stable stratification, and in case d), the temperature is uniform in the water layer. The heating-from-above experiments simulate some aspects of evaporation from natural bodies, like lakes, due to solar radiation. Evaporation rates were measured using a precision balance. Temperatures were measured in the water and in the ambient, and a thermal camera was used to monitor the water surface temperature and visualize the convection patterns. We present results of evaporation rates under the different conditions.

Peer-review under responsibility of Indian Institute of Technology, Hyderabad.

Keywords: Evaporation; Infrared

1. Introduction

Evaporation generally measured in mm/day is a globally studied phenomena starting from early 1900's. Ambient air temperature, relative humidity in air, water temperature & wind speed are the main factors which governs evaporation rates. Experiments have been carried out in oceans, lakes, rivers, swimming pools and other water

---

* Corresponding author. Tel.: +91-080-2293-2302;
E-mail address: navneetk@mecheng.iisc.ernet.in

Peer-review under responsibility of Indian Institute of Technology, Hyderabad.
doi:10.1016/j.piutam.2015.04.016

bodies to study evaporation at larger scales. Penmann [1] came up with an empirical correlation for evaporation rate in presence of a wind. There have been a few studies (Sharpley & Boelter [2], Boelter et al [3]) when there is no wind i.e. when evaporation occurs in a natural convection environment measured evaporation from a pan of water in natural convection environment. Goldstien [4] did some experiments on sublimation of naphthalene in planforms of different shapes inside a closed chamber. Recently Bowen & Saylor [5] have done experiments on evaporation from heated water placed in a container. They heated water to a particular temperature and then it was allowed to cool; cooling causes an unstable temperature gradient and thus convection. In natural systems like lakes and oceans, evaporation of water can occur due to absorption of sun's radiation. The IR component of the radiation is absorbed within a thin layer at the top. In these situations there may not be any convection in the water. In this paper we study evaporation from small tanks of water under conditions of no-convection (heating from above with an IR heater) and with natural convection (heating from below or cooling of heated water).

1.1. IR absorption spectrum of water:

Absorption spectrum of clean water has been a major topic of research recently. Though it started in the mid 1970's due to lack of proper instrumentation a deep knowledge in this field was lacking. But recently the science community has carried tremendous amount of research in this field. However their main aim was to study the behaviour of water at the molecular scale and understanding the nature of hydrogen bond. Now the absorption spectrum and penetration depth of a particular wave is well known and established. We in this study have used the fact that infrared radiations get absorbed within few thin (microns) layers of water. Thus these IR radiations do not penetrate much in clear water compared to visible radiations where the penetration depth can be of the order of several meters. Recently *Yves Marechal* [6] has studied the full IR spectrum of ordinary water, heavy water & combination of these at different temperatures. The maximum penetration depth according to him is 600nm at nearly 2900nm wavelength or 3400 cm^{-1} wavenumber. Figure 1 shows the absorption spectrum of water in IR range at working temperatures suitable for us. We use this fact to heat water in a tank from top. As mentioned earlier also the IR radiations get absorbed within very thin layers so they only heat these layers. Later on the depth wise temperature growth is purely dominated by conduction.

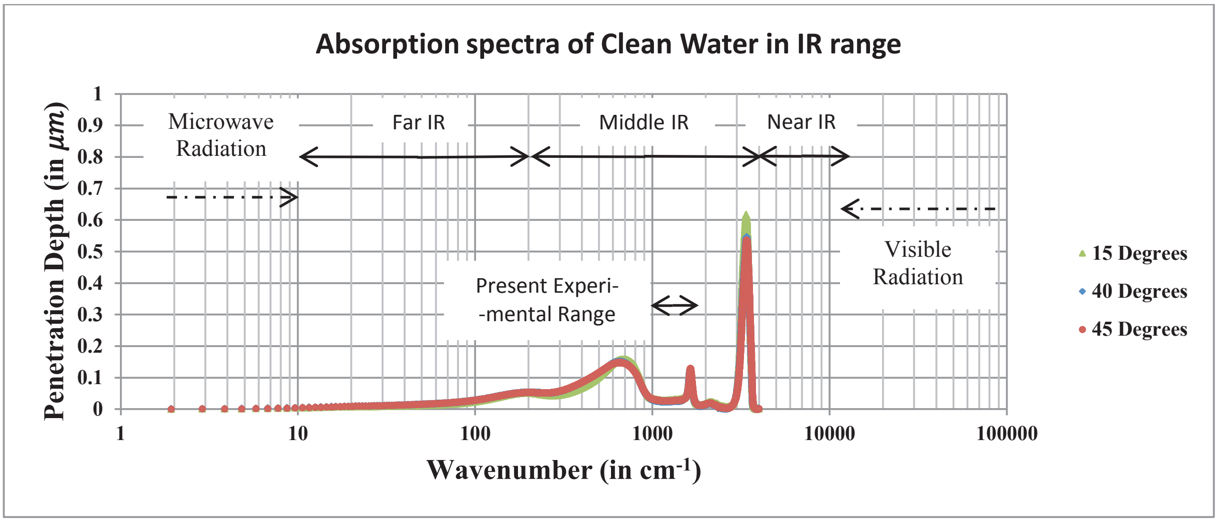

Fig: 1 Absorption spectrum of clean water in infrared range. Green, blue and red line corresponds to water temperatures of 15^0C, 40^0C and 45^0C respectively.

1.2. Wavelength Spectrum of Ceramic Infrared (IR) heater:

After exploring the IR absorption spectrum of water it becomes important to get a source which can emit these longwave radiations. The water temperature range in our studies is between 20^0C and 40^0C. Corresponding to these surface temperatures the IR heater temperature is between 35^0C (308^0K) and 250^0C (523^0K) as measured by the thermal camera for different distances between water surface and the ceramic IR heater. The peak wavelength according to the Wiens displacement law comes out to be between 9.75 μm and 5.74 μm and the wavenumbers are in the range 1000 cm^{-1} and 1750 cm^{-1}. Figure 2 shows the black body spectral distribution IR heater at different temperatures. For this range figure 1 shows the penetration depth of IR radiations in our experiments which was always below 200nm. We can now safely say that the process of heating from above using an IR heater is dominated by conduction.

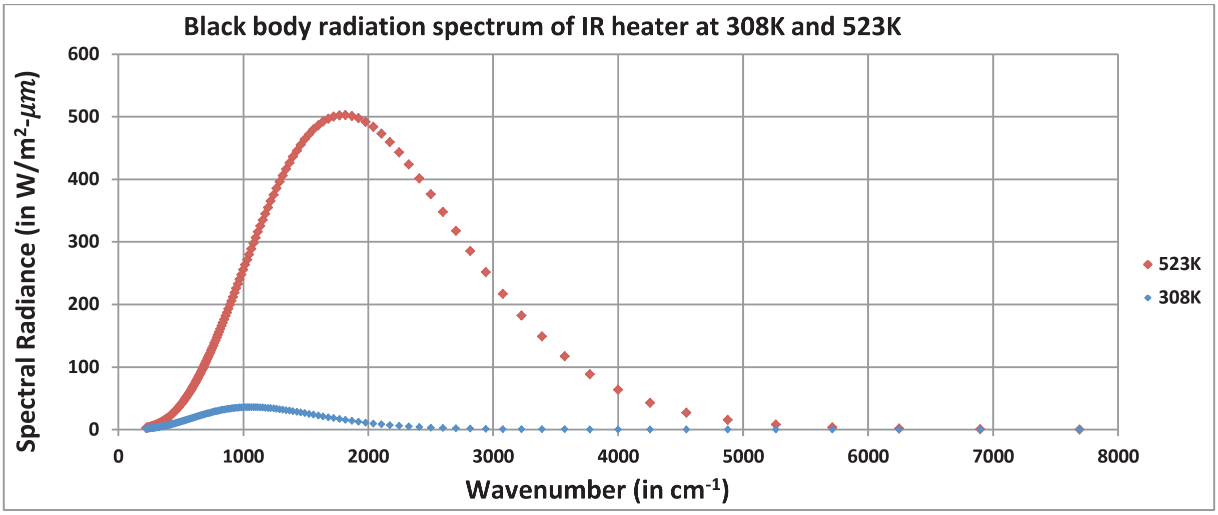

Fig: 2 Spectral radiance of ceramic IR heater at the two extreme temperatures encountered in the current set of experiments. Blue and red line represents 308^0K and 523^0K respectively.

1.3. Physical difference between heating from above and below:

Water needs energy to evaporate which it can take from the ambient. However heat sources like the sun speeds up the evaporation process by increasing the water surface temperature. As can be seen in figure 3, case (a) represents heating from above where the surface gets energy from the external source like the sun. This energy is then distributed among different components explained in figure 3(c). Figure 3(b) shows different types of energy associated when water surface is heated from below. Heating from below leads to convection in water once Rayleigh number crosses its critical value which is shown in figure 4(a). This water-side convection is absent in the case of heating from above as shown in figure 4(b). Typical temperature profiles are also shown for the two cases.

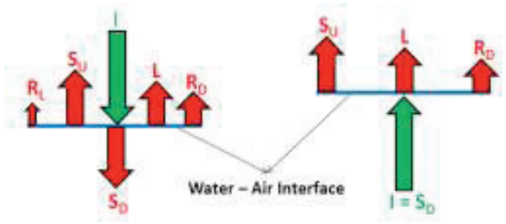

I = Incoming Radiation

R_L= Reflected Radiation

S_U = Sensible Heat (in air)

L = Latent Heat

R_D = Radiative Heat

S_D = Sensible Heat (in water)

(a) (b) (c)

Fig: 3 Pictorial representation of energy budget of the water-air interface in both cases, (a) heating from above and (b) Heating from below. The symbols are explained in (c)

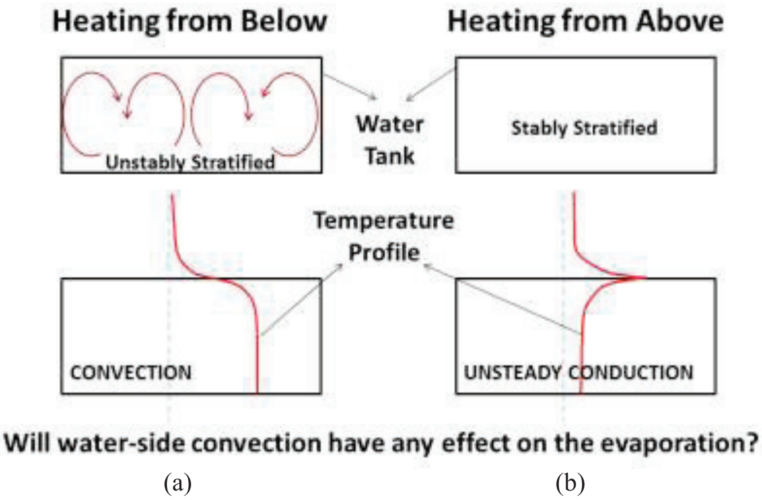

Fig: 4 Pictorial representation of water motion (in case of heating from below) and temperature profile in water and air for both cases, (a) heating from below and (b) Heating from above.

If one maintains the same conditions (Ambient temperature and ambient RH) and even same water temperature. The following questions can be asked:-

1) Will the evaporation rate be same in both the cases?
2) What is the effect of water-side convection on the evaporation rate?
3) What is the effect of temperature profile on the evaporation process?

In the present study we have tried to understand the whole process in detail and we will try to answer the above questions in the following sections.

1.4. Non-dimensional numbers:

1. Sherwood Number, $Sh = (h_m w)/D$
2. Rayleigh Number, $Ra = \frac{g\left(\frac{\Delta\rho}{\rho}\right)w^3}{\nu\alpha}$, for details of equations and terms refer to Bower & Saylor [5].

1.5. Calculation of Vapor Pressure Deficit (VPD):

Firstly we use the following empirical correlation to calculate saturated pressure (p):-

$$p = \frac{e^{77.3450 + 0.0057\,T - \frac{7235}{T}}}{T^{8.2}}, \qquad (1)$$

Here T (in K) can be both water surface temperature and the ambient temperature.

Once we get the saturated pressures p_w & p_a corresponding to T_w (water surface temperature) & T_a (ambient temperature) respectively using above equation, VPD is calculated as follows:-

$$\text{Vapor Pressure Deficit (VPD)} = p_w - (\text{RH})*p_a, \qquad (2)$$

Here RH is the relative humidity (in fraction) in the ambient. Fig 5 shows the variation of VPD with

$(\Delta T = T_w - T_a)$. It can be seen that VPD is a strong function of relative humidity (RH) and the non-linear nature of this curve makes matters even worse.

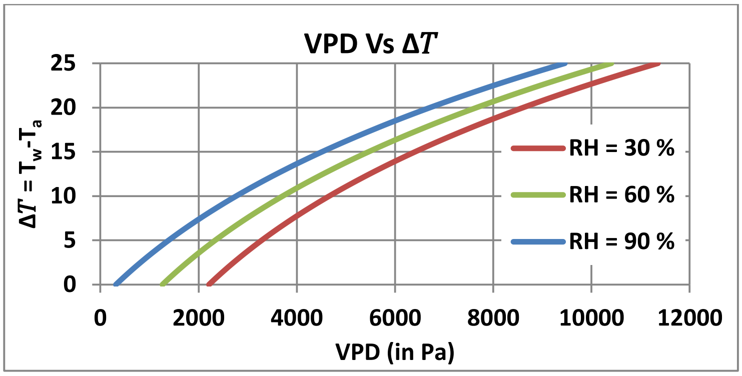

Fig.5 Variation of VPD with ΔT.Value of T_a has been fixed to 298K.

2. Experimental Setup

Experiments are conducted in two different tanks. Fig 6 shows the schematic of one of the type of experiment conducted in this study. One is a shallow brass tank of dimensions 15x15x1.2 cm and other is a deep glass tank of dimensions 18x18x10 cm. Water in the tank is heated either from above using a ceramic IR heater or from below using an immersion heater. Heating from above is studied for experiments in the brass tank. In case of glass tank both heating from above and below are studied. Evaporation from heated water as it cools is also studied.

Water loss is monitored through a precision weighing balance with resolution of 10 mg. Surface temperature is monitored though a thermal camera and T-type thermocouples are used to collect bulk water temperatures at different locations. A Honeywell humidity sensor, HIH-4000 is used to measure relative humidity (RH) in the ambient air. To measure ambient temperature thermocouples are used at different locations which are far away from both the evaporating tank and IR heater.

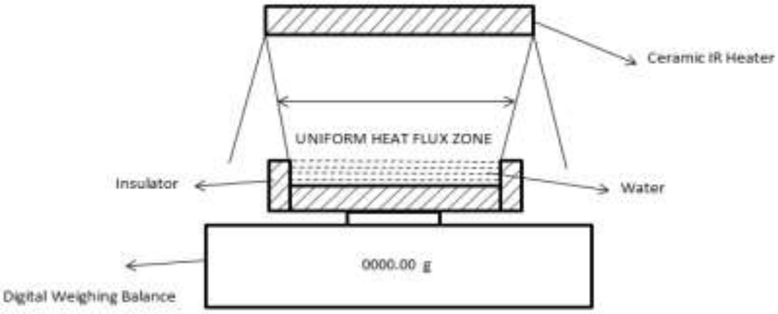

Fig.6 Schematic of the experimental setup.

3. Results and discussions

The different types of experiments have different behaviors as regards temperature variation with depth in the water and surface water temperature variation with time. Steady state is achieved in the shallow brass tank within 2.5 hours as can be seen in Fig 7(a) while heating from above. The entire layer of water and the tank are at the same temperature. Heating from above in the case of deep glass tank shows the quasi-steady nature of the process. In Fig 7(b) “Chan 113 (C)” in legend entry corresponds to thermocouple nearest to the surface. Based on the heat flux and thermal camera data we get the surface temperature. Fig 7(c) shows the temperature distribution in case of heating from below in the glass tank. Here also marked “Chan 113 (C)” thermocouple is nearest to the water surface.

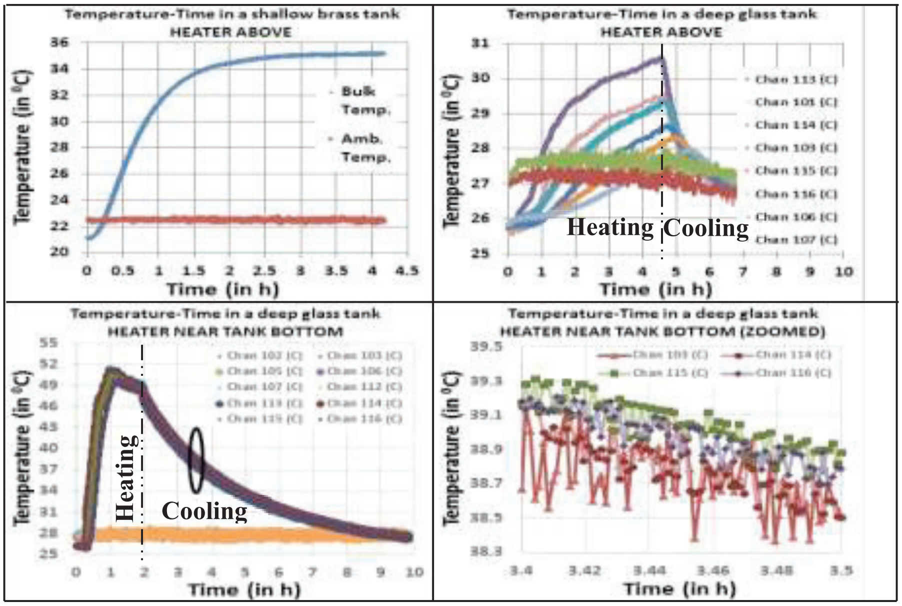

Fig. 7. (a) T-t curve in a shallow brass tank while heating from above using IR heater; (b) T-t curve in a deep glass tank while heating from above and allowed to cool using IR heater; (c) T-t curve in a deep glass tank while heating from below and allowed to cool and (d) zoomed image of (c) showing convection in the deep glass tank while heating from below. The vertical dashed line in (b) & (c) shows the demarcation between heating and cooling. The solid black ring in (c) represents the region selected to look for the temperature fluctuations as shown in (d).

After heating water for nearly 1 hour it is allowed to cool. Evaporation is a double diffusive phenomena; vapour pressure (VPD) deficit drives it. Fig 8(a) shows the variation of evaporation rate with VPD for all sets of experiments. It seems that even when the physical processes of heating from above and below are different at least on the water side there is no significant change in the evaporation rate at a particular VPD. The plot also shows linear dependency of evaporation rate on VPD which means the air resistance for water vapours remains same and is independent of other factors. Data is also transformed into the non-dimensional numbers. Sherwood number (Sh), a measure of evaporation rate is plotted against Rayleigh number (Ra) which is a measure of VPD as shown in Fig 8(b) where it is also compared to the correlation given by Bower & Saylor [5]. Our proposed power law $Sh = 0.264Ra^{0.292}$ is slightly different to the one proposed by Bower & Saylor [5] $Sh = 0.260Ra^{0.306}$.

The current investigation shows a difference of nearly 2-10 % in Sh between heating from above and below for same Ra. It says that there is possible difference in evaporation rates between heating from above & below. Our results are also within the error bar predicted by Bower & Saylor [5] where they used siphon technique to measure evaporation. It is possible that they might not have taken the effect of volume contraction in the evaporating tank while cooling into account which could lead to increased mass flow from the supply tank to the evaporating tank. It should also be noted that their predicted power law is a good fit for Ra>10^7 range. Absence and presence of water side convection can be seen in the thermal images in Fig 9. In Fig 9(a) (heating from above case) temperature across whole surface is more or less same. In 9(c) we can see very strong convection currents on the surface. Temperature data on a line drawn as shown in Fig 9(c) is plotted in Fig 10; drop in temperature corresponds to the presence of a cold plume. These cold plumes move about and merge with each other similar to what has been observed in RB convection. Merging rate of these cold plumes are reduced considerably when water is allowed to cool. Fig 9(d) shows the cold plumes when cooling starts after heating from below. The on-surface motion of the plumes are redu-

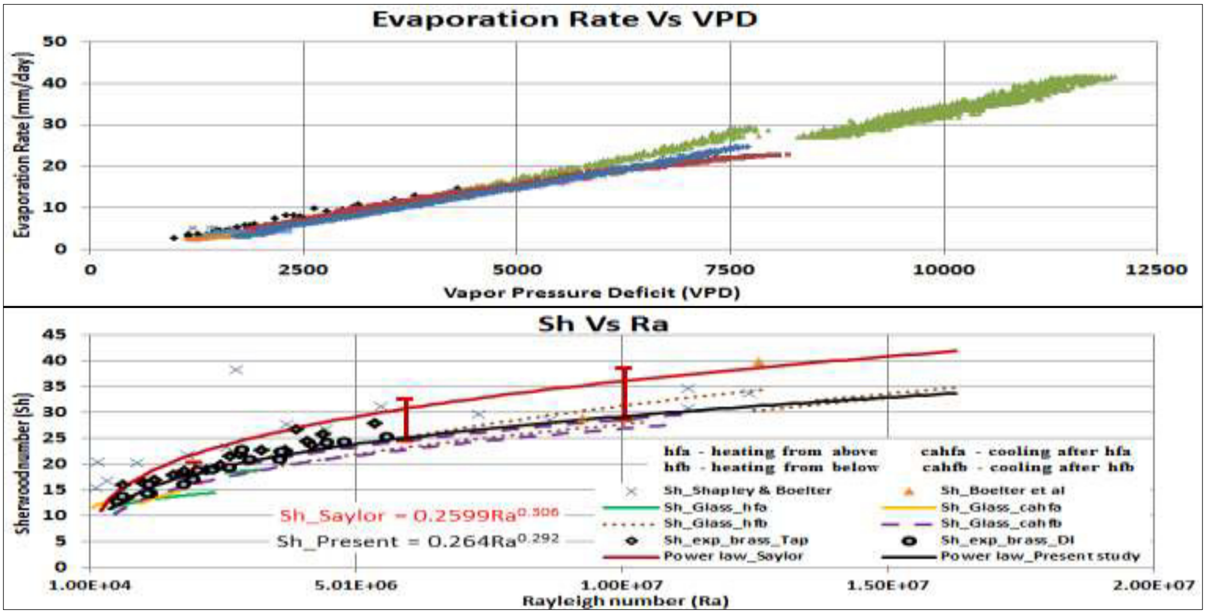

Fig. 8. (a) Evaporation Rate plotted with respect to vapor pressure deficit (VPD); (b) Sherwood number (Sh) versus Rayleigh number (Ra).

-ced compared to Fig 9(c). More organized structures can be seen when water is allowed to cool after heating from above. There is no convection in Fig 9(a) when heated from above as the water is stably stratified. Once cooling starts the surface water becomes cooler than water just below, leading to an unstable layer. Fig 9(b) shows convection in a thin upper layer which is laminar.

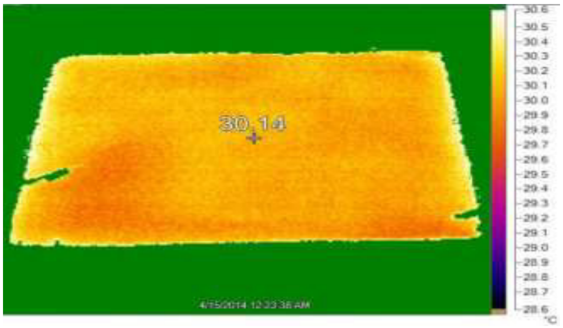

Fig 9(a) Thermal Image while heating from above.

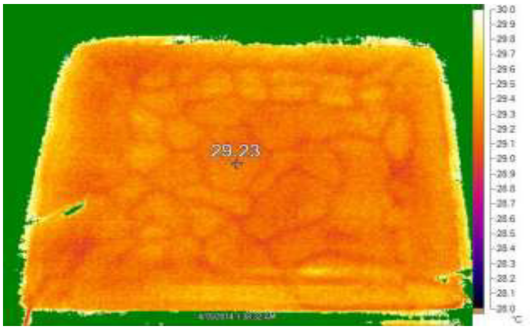

Fig 9(b) Thermal Image while cooling after heating from above.

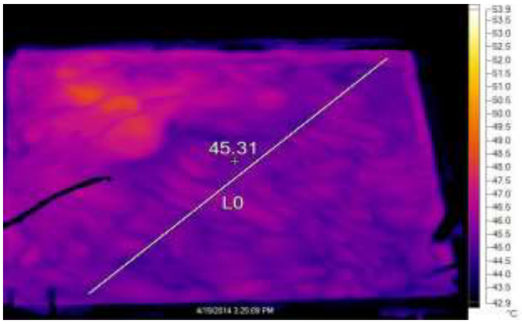

Fig 9(c) Thermal Image while heating from below.

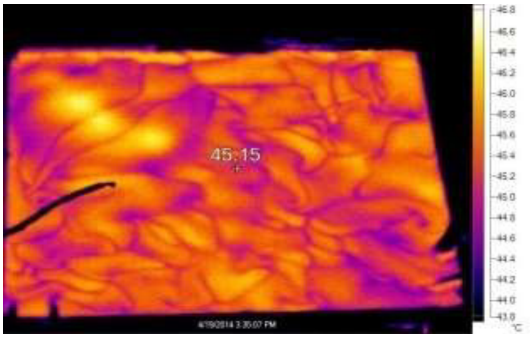

Fig 9(d) Thermal Image while cooling after heating from below.

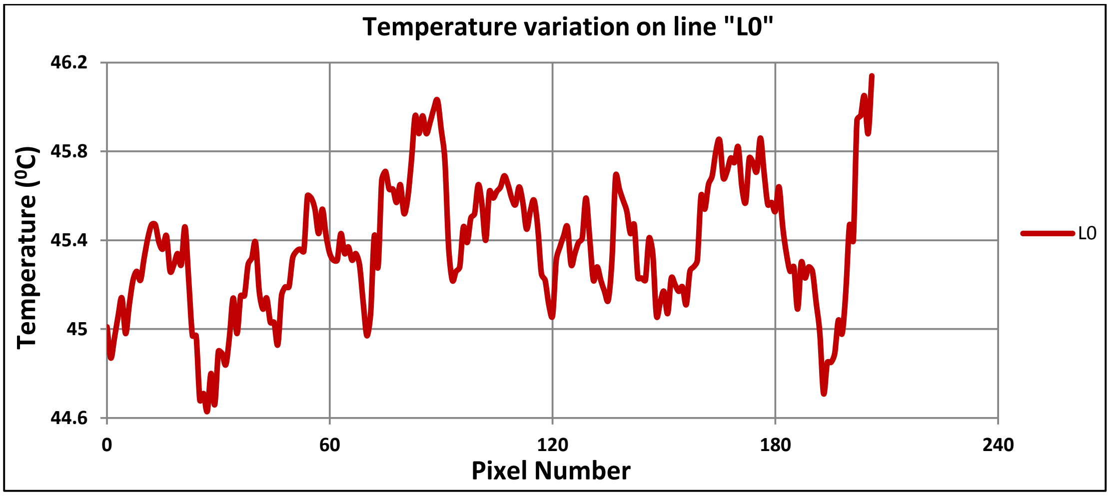

Fig 10 Pixel wise temperature data on a line marked “L0” shown in fig 8(c).

4. Conclusions

Experiments were conducted in different tanks filled with water undergoing natural convection-driven evaporation. Two ways of heating were used: 1) heating from above by an IR heater and 2) heating from below. Use of Infrared heater results in stable stratification and thus there is no convection in the water. Convection is dominant mode of heat transfer when water is heated from below. Heating from below or cooling of heated water results in convection in the water. In the shallow brass tank uniform steady temperature is achieved. Thermal imaging reveals formation of cold plumes, their merging and evolution with time. Evaporation rate, a critical parameter in meteorological sciences, was determined as a function of ambient temperature, water surface temperature and ambient relative humidity. A difference of 2-10 % in *Sh* was found in our experiments for same *Ra*. This difference could be within the error band of our experiments. But at first it seems water side convection does affect the evaporation process. These experimental data were also reduced to a dimensionless mass transfer coefficient for evaporation, *Sh*, and related to the Rayleigh number in air-side, *Ra* via a power law. The resulting Sh-Ra power law exponent was n=0.292 which is close to 1/3, a value similar to power law exponents obtained in many Nu-Ra studies of turbulent natural convection heat transfer including the Rayleigh-Benard convection.

References

1. Penman, HL. Natural evaporation from open water, bare soil and grass. *Proc Roy Soc London A* 1948; **194**:120-145.
2. Sharpley BF, Boelter LMK. Evaporation of water into quiet air from a one foot diameter surface.*IndEngChem*1938; **30**:1125–1131.
3. Boelter LMK, Gordon HS, Sharpley BF. Free evaporation into air of water from a free horizontal quiet surface.*IndEngChem*1946; **38**:596–600.
4. Goldstein RJ, Sparrow EM, Jones DC. Natural convection mass transfer adjacent to horizontal plates. *Int J Heat Mass Transfer* 1973; **16**:1025–1035.
5. Bower SM, Saylor JR. Erratum to A Study of Sherwood-Rayleigh relation for water undergoing Natural-Convection driven evaporation. *International Journal of Heat and Mass Transfer* 2009; **52**:3055-3063.
6. Marechal Yves. The molecular structure of liquid water delivered by absorption spectroscopy in the whole IR region completed with thermodynamics data. *Journal of Molecular Structure* 2011; **1004**:146-155.